# Electrical Current Flow and Cement Hydration: Implications on Cement-Based Microstructure

A. Susanto, G. Peng, D. A. Koleva, and K. van Breugel
Faculty of Civil Engineering and Geosciences, Delft University of Technology, Section of Materials and Environment, Stevinweg 1, 2628 CN Delft, Netherlands
Email: {a.susanto, P.Gao, D.A.Koleva, k.vanbreugel} @tudelft.nl

***Abstract*—Stray current is an electrical current "leakage" from metal conductors and electrical installations. When it flows through cement-based materials, electrical energy is converted to thermal energy that causes increasing temperature due to Joule heating phenomena. The aim of this paper is to shed light on the influence of electrical current flow on cement hydration, thermal properties and pore structure changes of cement-based materials. Calorimetry tests show that degree of cement hydration increases as a results of temperature increase due to electrical current flow through cement-based materials. To evaluate the influence of electrical current on the thermal properties of cement paste, the specific heat of cement paste was calculated based on the degree of cement hydration and temperature development during the hydration process. MIP tests were carried out to quantify changes in the pore structure due to electrical current flow. The results shows that if no other factors are present, leaching is avoided and for relatively early cement hydration age, the electrical current flow accelerates cement hydration, leading to an initial decrease in porosity of the cement paste.**

***Index Terms*—cement hydration, stray current, Joule heating, temperature, microstructure**

## I. Introduction

Cement hydration plays a critical role in the microstructural development of cement-based materials. Cement hydration is a complex exothermic chemical process, encompassing several phases which are linked to the contribution of different clinker minerals. The hydration process presents a series of chemical and physico-chemical reactions, accompanied by heat generation and heat evolution, which depend on cement composition, cement fineness, and ambient temperature as main factors [1], [2]. This process is a transformation from a high energy state to a lower one, where the energy is transmitted as heat [3]. During the cement hydration process, temperature rises as a result of the heat of cement hydration, which can be measured using e.g. thermocouples. Temperature is an important parameter which significantly affects materials properties and performance at early age, such as strength [4], [5], thermal stress [6] and distress (i.e. cracking) [7], [8]. The temperature development in a cement-based system is not only effected by the above-mentioned internal factors but also related to external factors (i.e. surrounding environment, stray current flow etc.). Stray current can flow in the surrounding medium through conductive paths and can therefore also flow through concrete and reinforced concrete structures.

The effects of stray current on steel corrosion in reinforced concrete are well recognized in the engineering practice. The effect of stray current on the bulk matrix alone is, however, is rarely considered and therefore scarcely reported. In fact, any electrical field, including stray current, influences cement hydration by altering ion and water transport. Consequently, electrical fields modify material properties and can affect the behavior and integrity of reinforced concrete as a global system. Therefore, stray current-related phenomena with relevance to both steel and concrete bulk properties are of high importance with respect to the service life of civil structures.

Stray current sources can be "supplied" from foreign Cathodic Protection (CP) installations, DC transit systems (e.g. electrified railways, subway systems, streetcars, welding operations, people movers), high voltage DC and electrical power transmission systems. Stray current tends to "enter" materials with low electrical resistance such as steel/reinforced concrete structures, water or gas pipeline, cable sheaths and any other buried metal installations. The effect of stray current depends on the level of the resulting current density. It has been reported that electrical current (including stray current) has negative effect on cement-based materials, for instance: 1) stray current can initiate and enhance steel corrosion [9]; 2) stray current alters microstructural properties of mortar and concrete bulk matrix [10]-[12]; 3) stray current has a significant influence on the degradation processes in cement-based systems [12] in terms of reduction in mechanical properties and increased permeability. Meanwhile, the effects of electrical current flow can be also positive at initial states e.g. for strength development of cement-based materials as within electrical curing application [13]-[16].

Among other effects, the electrical energy, as produced from stray current flow, converts to thermal energy, known as Joule Heating, and results in temperature rise in cement-based materials. The level of temperature rise is

Manuscript received September 17, 2016; revised November 17, 2016.



doi: 10.18178/ijscer.6.2.75-82

proportional to the square of the electrical current, flowing through the system [17]. The temperature rise, as produced by stray current flow, has the potential to increase the rate of cement hydration and consequently results in microstructural changes of the bulk cement-based matrix e.g. modified porosity, permeability, critical pore size. However, the influence of stray current flow on the hydration process and microstructural development of cement-based materials is not well understood.

Based on a series of experimental results, the aim of this work is to determine an "electrical enhancement" factor, which was further used as the correlation between temperature rise and electrical current flow through cement-based materials. A simulation approach to predict the temperature rise and subsequently altered cement hydration was employed. The simulation approach, using HYMOSTRUC3D, was validated through the recorded experimental data (e.g. isothermal calorimetry tests). Additionally, mercury intrusion porosimetry (MIP) tests were conducted to quantify relevant microstructural changes (porosity and pore structure) due to electrical current flow.

## II. Experimental Materials and Methods

### A. Materials

**Series A**: Cement paste and mortar prisms of 55 mm x 55 mm x 295 mm (Fig. 1a) were cast, using OPC CEM I 42.5N with water-to-cement ratio of 0.5 and cement-to-sand ratio of 1:3 for the mortar. The chemical composition (in wt. %) of CEM I 42.5N (ENCI, NL) is as follows: 63.9% CaO; 20.6% $SiO_2$; 5.01% $Al_2O_3$; 3.25% $Fe_2O_3$; 2.68% $SO_3$; 0.65% $K_2O$; 0.3% $Na_2O$. The specimens were maintained in semi-adiabatic conditions after casting and for the total test duration of 4 days. These specimens were used to monitor temperature alterations within cement hydration, with or without stray current involved, through embedded thermocouples.

**Series B:** Another group of mortar specimens i.e. mortar cubes of 40mm x 40 mm x 40 mm (Fig. 1b) were cast in the same manner and mix design. They were maintained in sealed conditions for test duration of 112 days. The mortar cubes were subjected to some of the lower current density regimes (as specified further below).

**Series C**: Cement paste, w/c ratio 0.35 and 0.5 with weight 10 ± 0.01g samples was cast for isothermal calorimetry test.

### B. Sample Designation

*1) Series A – specimens with embedded thermocouples:*

Two main groups of specimens were investigated: 1) Control (reference) group - no DC current involved and 2) Stray current group with subgroups, reflecting the level of DC current involved i.e. groups "1 A/m$^2$", "10 A/m$^2$", "40 A/m$^2$", and "60 A/m$^2$". The set-up for DC current application is as depicted in Fig. 1a.

*2) Series B – sealed mortar cubes: the specimens were presented by three sub-groups:*

1) control group - no DC current involved; 2) group "100 mA/m$^2$" and 3) group "1A/m$^2$" (Fig. 1b).

*3) Series C – cement paste used for isothermal calorimetry tests:*

The tests were performed on three groups of samples: control group, "10 mA/m$^2$", "100 mA/m$^2$" and "1A/m$^2$" group. The experimental set up of calorimetry tests is presented in Fig. 2.

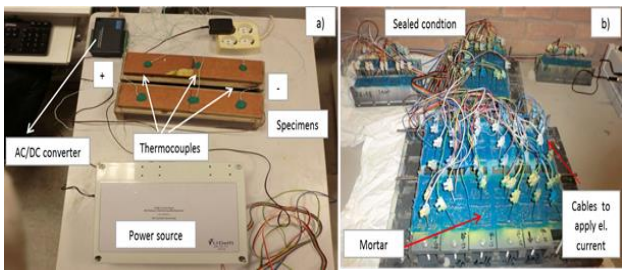


Figure 1. Experimental set-up for measurements of temperature increase in cement paste and mortar specimens due to electrical current flow (Series A) (a) and experimental set up of electrical current flow through mortar specimens in sealed condition (Series B) (b).

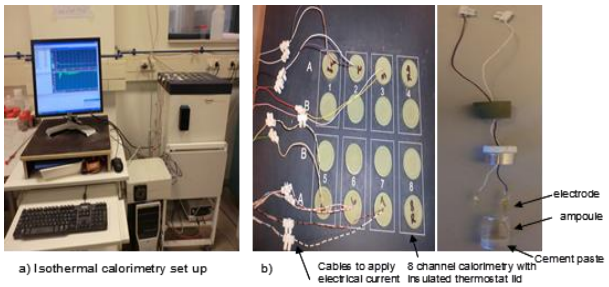


Figure 2. (a) Isothermal calorimeter (TAM-Air-314) used to measure heat release of cement paste; (b) Schematic pictures of the holders for "under current" regime (Series C).

### C. Current Regime

A simulation of stray current was achieved by applying a DC current at the level of "1 A/m$^2$", "10 A/m$^2$", "40 A/m$^2$", and "60 A/m$^2$". For the specimens in Series A, a negative and a positive terminal were connected to a 80 V source. The current density levels were adjusted by additional resistors. The relevant surface area was calculated based on the geometry of the specimens, essentially the cross section A (i.e. A=55 mm x 55 mm). Thermocouples were placed immediately after casting of the cement paste (and mortar) to record automatically the temperature development by connecting to the AC/DC converter and the personal computer (PC). For the specimens in Series B, DC current was applied with level of 100mA/m$^2$ and 1A/m$^2$. For the specimens in Series C, DC current was applied with level of 10mA/m$^2$, 100mA/m$^2$ and 1A/m$^2$.

### D. Isothermal Calorimetry Tests

Heat evolution and rate of hydration of cement paste were measured by Thermometric isothermal conduction calorimeter (TAM-Air-314, an 8-channel heat flow calorimeter). The specimen preparation and experimental procedure followed well known methodology [18], except for the modifications related to the application and

monitoring the effect of electrical current flow. For the "under current" samples, the same ampoules as for the control cases were used, but designed in a way to include two metal electrodes as electrical current conductors (schematic pictures in Fig. 2b). Electrical current was applied immediately after samples' casting from an external source for about 7 days.

### E. Temperature Development

To simulate stray current, an electrical field was applied to the cement-based specimens (paste and mortar prisms) immediately after casting and until approximately 4 days of age. The temperature increase due to both cement hydration and electrical current flow were measured for the specimens in Series A, using thermocouples, embedded in the middle, right and left sections of the specimens (Fig. 1a).

### F. Mercury Intrusion Porosimetry (MIP)

MIP was performed for the specimens in Series B in order to characterize porosity changes in the bulk matrix due to stray current flow. The sample preparation for MIP tests followed generally accepted and reported procedure [19]-[21], i.e. drying treatment to removes of water from the sample before mercury pressure is applied. For isothermal calorimetry tests, MIP was conducted for cement paste at hydration age of 7 days.

### G. Compressive Strength

The specimens from Series B – mortar cubes – were subjected to compressive strength tests, recorded at 3, 7, 28, and 112 days. Hereby reported are the results for hydration ages 4, 8, 29, and 113 days as relevant to this work.

## III. Results and Discussion

### A. Degree of Cement Hydration

Based on the isothermal heat of hydration that was derived from integration of the rate of heat evolution, the degree of hydration at time *t* can be calculated using the following equation [22], [23]:

$$\alpha = \frac{Q(t)}{Q_{\max}} \tag{1}$$

where Q(t) is the heat liberated at time t (J/g), $Q_{max}$ is the maximum amount of heat liberated at complete hydration (J/g).

Due to electrical current flow through the specimens, maximum amount of heat liberated at complete hydration is calculated as follows:

$$Q_{\max} = (Q_{\max})_{cem} + (Q_{\max})_{el} \tag{2}$$

where $(Q_{\max})_{cem}$ is maximum heat of hydration of Portland cement at complete hydration (J/g), $(Q_{\max})_{el}$ is the maximum amount of heat liberated by electrical current flow at complete hydration (J/g).

Calculation of maximum heat of hydration of Portland cement $(Q_{\max})_{cem}$ has been proposed by Verbeek [23]:

$$(Q_{\max})_{cem} = q_1.(C_3S) + q_2.(C_2S) + q_3.(C_3A) + q_4.(C_3AF) + q_5.(C) + q_6.(M_gO) \tag{3}$$

where $q_1..q_6$ are the heat of hydration of the constituents considered.

The maximum amount of heat liberated by electrical current flow $(Q_{\max})_{el}$ can be calculated using the following equation:

$$(Q_{\max})_{el} = \frac{1}{m_c}\int_0^{\tau} I^2 R\,dt \tag{4}$$

where I is the electrical current flow (in Ampere), R is the resistance of cement (in Ohm), τ is the final time (in second) and $m_c$ is the mass of cement (in kg).

Fig. 3 reveals the effect of electrical current flow on the heat release and the degree of hydration of cement paste, determined by isothermal calorimetry at 20°C curing with w/c ratios 0.35 and 0.5. The results show that the heat release of cement paste in condition of stray current flow is comparable to the control cement paste. However, the stray current flow promotes additional heat release. The extra amount of heat release can be explained by conversion of electrical energy to thermal energy that can be quantified by temperature development of cement paste. As seen in the Fig. 3a the main peak of heat release occurs at about 12 to 14 hours after casting. As the electrical current density increases, the acceleration peak of the heat release curve for the current regime specimens shifts to shorter time intervals, which means slightly accelerated cement hydration. These peaks can be associated to the $C_3S$ hydration [2], [3] which occurs earlier for the current regimes, compared to control specimens. In addition, the intensity of this peak is greater if the water-to-cement ratio is lower (i.e. 0.35)

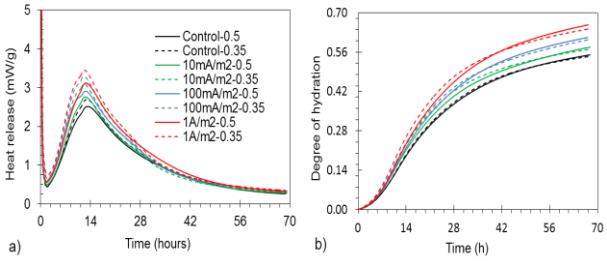


Figure 3. Heat released (a) and degree of hydration (b) as function of time for cement paste with w/c 0.5 and 0.35.

Generally, the degree of cement hydration for w/c ratio 0.35 is slightly higher at early age and up to about 42 hours. After this period, slightly lower values were recorded, from 42 hours to the end of the test, compared to results in specimens of w/c ratio 0.5. The higher degree of cement hydration for specimens of w/c ratio 0.5 at the later ages, compared to these of w/c ratio 0.35, is a consequence from the larger amount of water available for cement hydration. This results in more space, available for the dissolution of reactants, nucleation and precipitation of hydration products, as stated by Bentz [24], [25]. At higher temperature, the degree of hydration initially develops faster but ends up with lower ultimate values at later stages [26]-[28] – a result, also confirmed through the outcomes of this study.

### B. Rate of Cement Hydration in Condition of Stray Current Flow

The rate of cement hydration was derived from the Arrhenius equation:

$$k_2 = k_1 \exp\left\{\frac{E_a}{R}\left(\frac{1}{T_1}-\frac{1}{T_2}\right)\right\} \quad (5)$$

where $k_1$ is the specific reaction velocity (rate constant) at $T_1$ and $k_2$ is the specific reaction velocity at $T_2$. In this case, $k_2$ is the specific reaction velocity due to electrical current flow at $T_2$ which is the temperature increase due to electrical current flow.

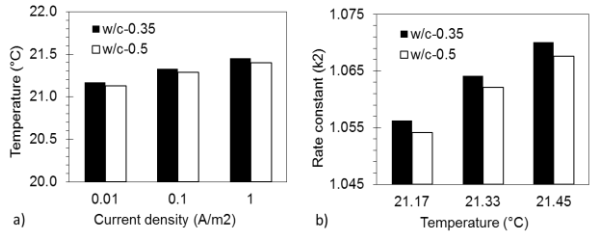


Figure 4. Temperature increase as function of electrical current density (a) and rate constant as function of electrical current density (b) in cement paste compared to control specimens.

Based on the relationship between temperature and the specific reaction velocity, it is possible to calculate the rate of hydration in cement-based materials due electrical current flow (Eq. (5)). In the temperature range above 20 ℃, the activation energy ($E_a$) for ordinary Portland cement may be assumed to be 33.500J/mol [29] By solving Eq. (5), it follows that at w/c ratio 0.35 the increase of temperature is from 21.29 ℃, to 21.42 ℃, 21.55 ℃ (due to application of electrical current with level current density 10 mA/m$^2$, 100 mA/m$^2$ and 1A/m$^2$, respectively). This means increase of hydration rate by factor of 1.056, 1.064, and 1.070, respectively (see Fig. 4b). Whereas for w/c ratio 0.5, the increase of temperature is from 21.25 ℃, 21.38 ℃, 21.54 ℃ (Fig.4a), increasing hydration rate by factor of 1.054, 1.062, and 1.068, respectively (see Fig. 4b). It can be seen in Fig. 4b that the rate of cement hydration strongly depends on the level of electrical current and the w/c ratio.

### C. Pore Structure of Cement Paste

Fig. 5 depicts the porosity changes (derived from MIP) of cement paste due to electrical current flow. As shown in Fig. 5, total porosity is reduced with increasing the level of electrical current and with lowering the w/c ratio. In the case of "under current" regimes, the hydration products would be formed faster, surrounding the hydrating cement particles, resulting in a denser gel due to a larger amount of hydration product. In other words, the porosity of cement paste decreases with increased percentage of hydration products. For "under current" regimes with w/c ratio 0.35, the total porosity decreased to 0.55%, 2.61%, and 4.26% for current density levels of 10mA/m$^2$, 100mA/m$^2$ and 1A/m$^2$, respectively, compared to control specimens. For specimens of w/c ratio 0.5, these numbers are slightly smaller i.e. 0.53%, 2.34%, 3.41%, respectively. This different effect may be caused by the fact that higher w/c ratio would results in a higher total porosity as pointed out by Odler *et al*. [30] and confirmed by other authors [31]-[33].

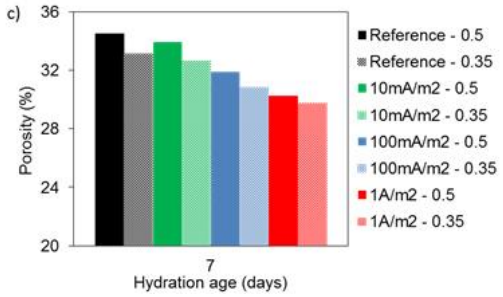


Figure 5. Total porosity development of cement paste

The influence of electrical current flow on temperature increase in cement paste and mortar was simulated by employing various already reported equations [34]: the electrical current flow through cement paste (and mortar) increases the temperature development due to resistive heating, or Joule heating effect, resulting in accelerating the rate of cement hydration. In HYMOSTRUC3D, the penetration rate of the reaction front for an individual cement particle at time t is computed with the following basic rate formula [22].

$$\frac{\Delta\delta_{in;x,j+1}}{\Delta t_{j+1}} = K_o * F_1(.) * \Omega_1(.) * \Omega_2(.) * \Omega_3(.) * \left[\left(\frac{\nu(T_j)}{\nu_{tr}(T_j)}\right)^{\beta_2} * \left\{\left(\frac{\nu(T_j)}{\nu_{20}}\right)^{\beta_2} * \frac{\delta_{tr,20}}{\delta_{x,j}}\right\}^{\beta_1}\right]^{\lambda} \quad (6)$$

where $K_o(.)$ is the basic rate factor (μm/h), $F_1(.) = F_1(T_j, \alpha_j, C_3S)$ , $\Omega_1(.) = \Omega_1(x, \alpha_{x,j})$ , $\Omega_2(.) = \Omega_2(\alpha_j)$ and $\Omega_3(.) = \Omega_3(\alpha_j)$.

The influence of electrical current flow on temperature increase in cement paste can be incorporated through temperature functions in Equation 7, namely $F_1$ and $F_2$. $F_1$ $(T,\alpha,C_3S)$ is the Arrhenius function that quantifies the effect of the curing temperature T on the rate penetration of reaction front in an individual cement particle:

$$F_1(T,\alpha,C_3S) = A * \exp\left(-\frac{AE\ (T,\alpha,C_3S)}{R*(273+T)}\right) \quad (7)$$

where R is the gas constant (8.31 10$^3$ kJ/mol.K), A is the constant and AE is the activation energy.

Whereas $F_2$ is accounted for the effect of temperature-induced morphological and structural changes that can be represented by the following equation:

$$F_2(T) = \left(\frac{\nu(\tau)}{\nu_{20}}\right)^{\beta_2} \quad (8)$$

With $\nu(T) = 2.2 * e^{-28.10^{-6}\tau^2}$ and $\nu 20 = \nu(T_{20})$

where T is the isothermal temperature, $\overline{T}$ is the weight temperature which is the mean temperature in the hydration domain.

To determine an appropriate model for temperature rise in condition of electrical current flow, curve fitting from experimental data were performed using log normal distribution function as follows:

$$T(t) = T_0 + \left(\frac{A}{\sigma}\right)\left(0.000102\left(\frac{J}{J_u}\right)^2 + 0.01025\frac{J}{J_u} + 0.95\right) * \frac{1}{t\sqrt{2\pi}} \exp\left(-\frac{\left[\ln\frac{t}{\mu}\right]^2}{2\left(0.0014\frac{J}{J_u} + 0.471\right)^2}\right) \quad (9)$$

where $T_o$ is the initial temperature (℃), A is the constant, J is the electrical current density ($A/m^2$), $J_u$ is the unit of electrical current density ($A/m^2$).

## IV. Simulation Results and Discussion

In this section, simulation of the hydration of Portland cement with four-phase concept is discussed and validated with experimental results. The size of the simulated cubic cement paste is 100 µm x 100 µm x 100 µm. Based on Eq. (9) an approximated relationship between the applied electrical current density and the temperature development of cement paste, as given in the Fig. 6, can be derived. Furthermore, from Eq. (9) the level of current density, able to substantially increase the temperature and therefore to possibly create internal damage can be predicted, which is as aforementioned at temperatures higher than 60°C. By considering 60°C as a threshold of positive vs negative effects of the current flow, the corresponding electrical current density value is $300 A/m^2$ (derived by solving of Eq. (9)). This means that when electrical current flow through the cement paste is higher than 300 $A/m^2$, the maximum temperature increase in cement paste is higher than 60°C and the potential to create internal damage is high.

### A. *Effect of Low Level Current Density (≤ 1A/m2) on Degree of Cement Hydration*

Fig. 7 presents simulation of the accelerated degree of cement hydration as dependent on the level of temperature rise due to electrical current flow, validated with isothermal calorimetry tests. The influence of temperature rise due to electrical current flow on the degree of hydration and hydration product is governed by Arrhenius function, $F_1$, in Eq. (7) and $F_2$ in Eq. (8) that quantifies the effect of the curing temperature on the rate penetration of reaction front in an individual cement particle. This controls the temperature-induced morphological and structural changes, respectively.

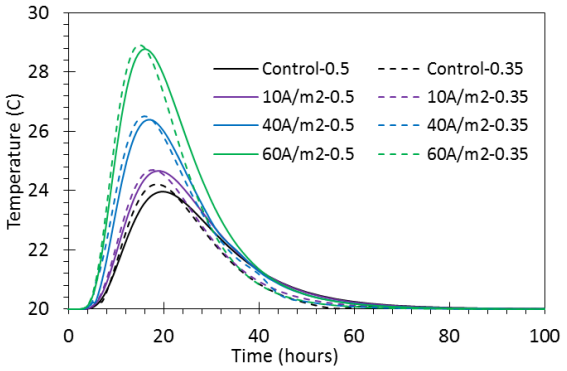


Figure 6. Relationship between applied electrical current density and temperature development of cement paste.

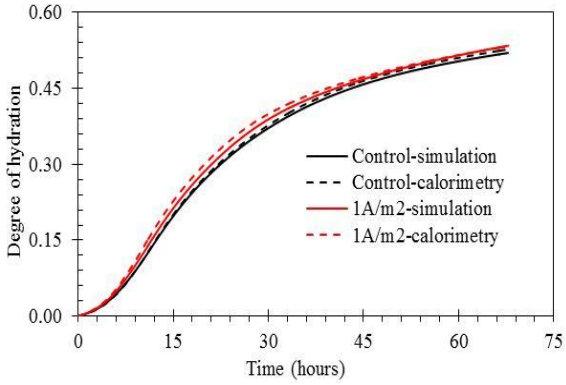


Figure 7. Simulation of degree of hydration as function of time for cement paste with w/c 0.5 and validation with experimental data from calorimetry tests.

As seen in the Fig. 7, $1A/m^2$ current density is enough to accelerate the degree of cement hydration compared to control specimens, even if the temperature rise due to electrical current flow is quite small - about 1.54 ℃ from 20 ℃ to 21.54 ℃ (Fig. 4a). The simulation results have a good agreement with experimental results (Fig. 7). For example, the accelerated cement hydration in condition of stray current flow was confirmed by MIP tests (Fig. 5).

### B. *Effect of Higher Level Current Density (>1A/m2) and Varying w/c Ratio on Degree of Cement Hydration*

The simulation results in Fig. 8 show that degree of hydration of cement paste for w/c ratio 0.35 tends to have higher values at early age but lower values at later age compared to w/c ratio 0.5 (Fig. 8). This is due to the fact that less water in the low water to cement ratio will be heated by electrical current flow faster, resulting in accelerated kinetics of cement hydration at early age. However, specimens with higher w/c ratio (i.e. 0.5) generally exhibit a higher degree of hydration than the lower w/c ratio (i.e. 0.35) at later age as also stated by Bentz [35]. As has been mentioned earlier, this is due to the larger volume of water, available for cement hydration at higher w/c ratios. Furthermore, it can be seen, Fig. 8, that the degree of cement hydration increases as the intensity/level of electrical current flow increases.

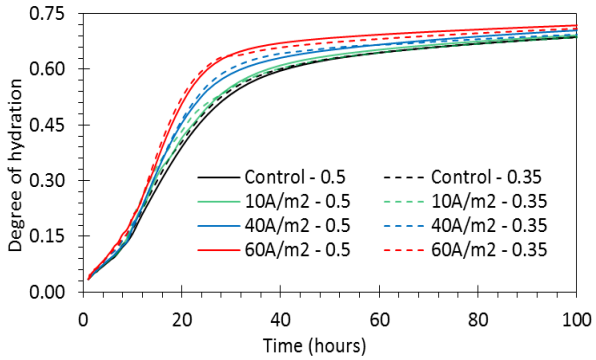


Figure 8. Degree of hydration of cement paste with different level electrical current density as function of time.

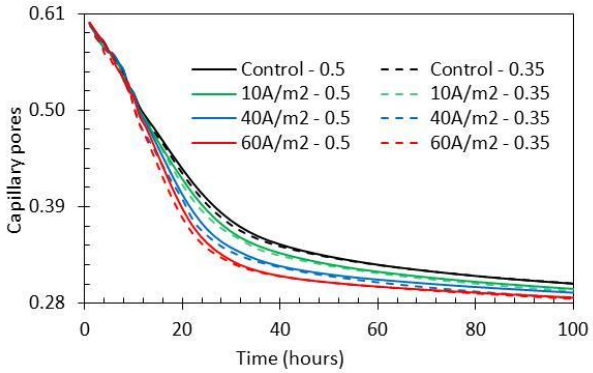


Figure 9. Capillary pores development of cement paste in condition of electrical current flow as function of time

Fig. 9 reveals capillary pores development of cement paste in condition electrical current flow as function of time. The results are derived from the HYMOSTRUC3D simulation. Generally, porosity decreases as the hydration proceeds. In addition, the porosity of a paste with lower level electrical current flow is greater than the porosity of the same paste with higher level electrical current. Similar results were obtained from Goto et al. study [36] in which they investigated the effect of w/c ratio (i.e. 0.35, 0.40, 0.45) and temperature (i.e 27 ℃ and 60 ℃) on total porosity of a cement paste at 28 days. However, the hydration proceeds, the effect of electrical current flow on porosity becomes less evident because the effect of electrical current flow on the ultimate degree of hydration is small (see Fig. 8).

### C. Nu-Factor

Fig. 10 reveals the ν-factor development of paste as function of time. The ν-factor gives the ratio between volume of the reaction products and volume of the reactant.

As seen in the Fig. 10 the nu-factor of paste gradually decreases with increasing the electrical current flow at early age (< 40 hours). A decrease of the nu-factor corresponds to accelerated degree of cement hydration (see Fig. 10). The consequence of a decrease of nu-factor on the rate of reaction has been investigated by some authors [22], [37]. Two of the various reasons for this phenomenon are as follow: (a) with decreasing value of v, the thickness of the product layer decreases. A thinner layer implies a lower diffusion resistance and hence an increase in the rate of reaction b) with decreasing value of v the density of the product layer increases. This enhances the diffusion resistance of the product layer and will cause a decrease in the rate of reaction. After 40 hours of cement hydration, the nu-factor tends to increase with increasing the level of electrical current flow. The effect was more pronounced for the higher level of current density.

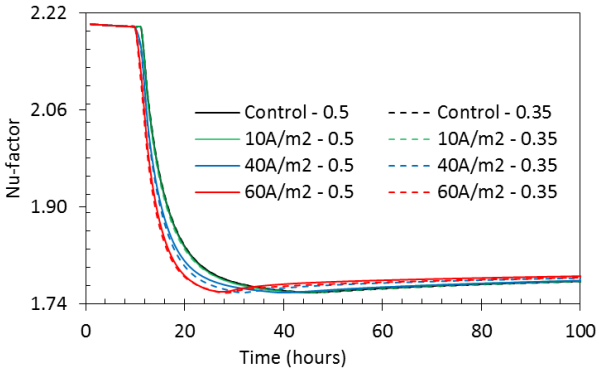


Figure 10. Nu-factor development of paste as function of time

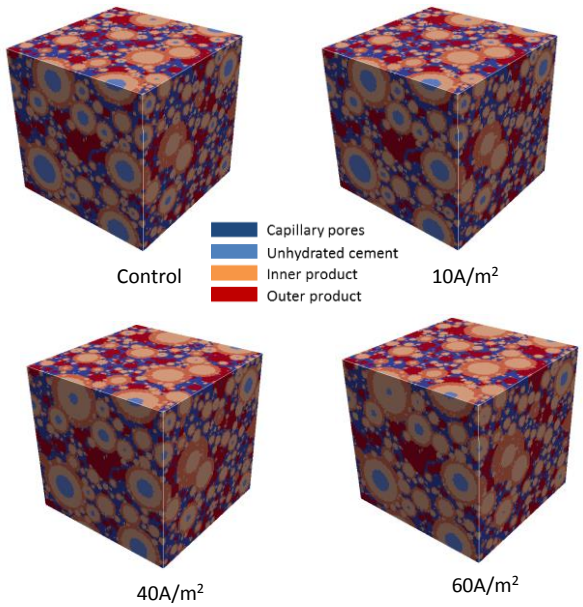


Figure 11. 3D microstructure of cement hydration at different level electrical current flow with water-to-cement ratio 0.5.

### D. Virtual 3D Microstructure

In order to quantify the influence of electrical current flow on the hydration products of cement paste, HYMOSTRUC3D simulations were performed. Figure 11 shows the virtual 3D microstructure of hydrated cement paste at different levels of current density with two different water-to-cement ratio (i.e. 0.5 and 0.35). Fig. 11 presents the simulation for w/c ratio 0.5 only. The dimension of the simulated 3D volume of cement paste microstructure is 100x100x100 $\mu m^3$. The enhanced cement hydration due to electrical current flow was already experimental recorded. This leads to re-distribution of hydration products in the cement paste. The modelled microstructure of cement paste, hardly changes at levels of electrical current, lower than 60 $A/m^2$

(Fig. 11). There was no significant difference of hydration products distribution. At the level of 60A/m$^2$, accelerated cement hydration was already more obvious. The simulation results are well in line with the experimentally derived results. Therefore, the employed numerical simulation can be further employed to derive microstructural changes in the presence of significantly larger current density levels.

## V. Conclusions

This paper deals with the influence of electrical current flow on cement hydration and microstructural changes of cement paste. The experimental results were coupled to simulation of the process of hydration. The following conclusions can be drawn:

1. Temperature increase due to electrical current flow accelerates cement hydration, leading to increase in the amount of hydration products in the cement paste. The level of temperature increase is proportional to the square of electrical current flow in the cement-based materials.
2. Temperature increase in cement-based materials due to electrical current and its effect on performance depend on several factors, as follows:
   a) initial properties of the cement paste (e.g. w/c ratio);
   b) cement content;
   c) level of the electrical current flow;
3. The specific heat of cement paste decreases with increasing the level of electrical current flow and with increasing the w/c ratio.
4. Numerical simulation of the hydration process is well in line with the experimental results and can be employed further to elucidate similar mechanisms in various conditions as different w/c ratio or higher current density levels.

## References


[1] P. C. Hewlet, *Lea's Chemistry of Cement and Concrete*, 4th ed. Oxford: Butterworth-Heinemann, 2004.
[2] H. F. P. Taylor, *Cement Chemistry*, 2nd ed. London: Thomas Telford, 1997.
[3] S. Mindess, J. F. Young, and D. Darwin, *Concrete: Prentice-Hall*, Upper Saddle River, New Jersey, USA, 2003.
[4] W. M. Hale, T. D. Bush, B. W. Russell, and S. F. Freyne, "Effect of curing temperature on hardened concrete properties," *Transportation Research Record: Journal of the Transportation Research Board*, no. 1914, pp. 97–104, 2005.
[5] R. C. Tank, "The rate constant model for strength development of concrete," Ph.D. Dissertation, Polytechnic University, Brooklyn, New York, 1988.
[6] H. T. Yu, L. Khazanovich, M. I. Darter, and A. Ardani, "Analysis of concrete pavement responses to temperature and wheel loads measured from instrumented slabs," *Transportation Research Record*, no. 1639, pp. 94–101, 1998.
[7] T. Nishizawa, T. Fukuda, S. Matsuno, and K. Himeno, "Curling stress equation for transverse joint edge of a concrete pavement slab based on finite-element method analysis," *Transportation Research Record*, no. 1525, pp. 35–43, 1996.
[8] A. R. Mohamed and W. Hansen, "Effect of nonlinear temperature gradient on curling stress in concrete pavements," *Transportation Research Record: Journal of the Transportation Research Board*, no. 1568, pp. 65–72, 1997.
[9] L. Bertolini, M. Carsana, and P. Pedeferri, "Corrosion behaviour of steel in concrete in the presence of stray current," *Corrosion Science*, vol. 49, pp. 1056-1068, 2007.
[10] D. A. Koleva, J. H. W. de Wit, K. van Breugel, L. Veleva, E. P. M. van Westing, O. Copuroglu, and A. L. A. Fraaij, "Correlation of microstructrure, electrical properties and electrochemical phenomena in reinforced mortar. Breakdown to multi-phase interface structures. Part II: Pore network, electrical properties and electrochemical response," *Materials Characterization*, vol. 59, pp. 801-815, 2008.
[11] D. A. Koleva, K. van Breugel, and J. H. W. de Wit, "The effect of electrical current flow, as a simulation of cathodic prevention, on early hydration rate and microstructure of cement-based materials," European Federation of Corrosion, no. 299, 2008.
[12] A. Susanto, D. A. Koleva, and K. van Breugel, "DC current-induced curing and ageing phenomena in cement-based materials," in *Proc. 1st International Conference on Ageing of Materials and Structures*, Delft: Ageing Center TU Delft, pp. 562-568, 2014.
[13] S. Bredenkamp, D. Kruger, and G. L. Bredenkamp, "Direct electric curing of concrete," *Magazine of Concrete Research*, vol. 45, no. 162, pp. 71-74, March 1993.
[14] L. Heritage, "Direct electric curing of mortar and concrete," Napier University, Edinburgh, UK, 2001.
[15] G. W. John and K. G. Narendra, "Equipment for the investigation of the accelerated curing of concrete using direct electrical conduction," *Measurement*, vol. 35, pp. 243–250, 2004.
[16] J. G. Wilson and N. K. Gupta, "Analysis of power distribution in reinforced concrete during accelerated curing using electroheat," *IEE Proceedings–Electric Power Applications*, vol. 143, no. 2, pp. 172–176, 1996.
[17] A. von Meier, *Electric Power Systems: A Conceptual Introduction*, p. 67, 2006, John Wiley & Sons, USA.
[18] L. Wadso, "An experimental comparison between isothermal calorimetry, semi-adiabatic calorimetry and solution calorimetry for the study of cement hydration," NORDTEST Report 522, 2003.
[19] M. S. Sumanasooriya and N. Neithalath, "Stereology- and morphology-based pore structure descriptors of enhanced porosity (previous) concrete," *ACI Materials Journal*, vol. 106, no. 5, pp. 429-438, 2009.
[20] J. Hu, "Porosity of concrete, morphological study of model concrete," PhD thesis, Delft University of Technology, Delft 2004.
[21] G. Ye, "Experimental study and numerical simulation of the development of the microstructure and permeability of cementitious materials," Ph.D. thesis. Delft: Delft University of Technology, 2003.
[22] K. van Breugel, "Simulation of hydration and formation of structure in hardening cement-based materials," PhD thesis, Delft University of Technology, the Netherlands, 1991.
[23] G. J. Verbeek, *4th ISCC*, Washington, Paper IV-3, pp. 453-465, 1960.
[24] D. P. Bentz, "Three-dimensional computer simulation of Portland cement hydration and microstructure development," *J. Am. Ceram. Soc.*, vol. 80, no. 1, pp. 3–211, 997.
[25] D. P. Bentz, "Influence of water-to-cement ratio on hydration kinetics: Simple models based on spatial considerations," *Cement and Concrete Research*, vol. 36, pp. 238–244, 2006.
[26] Y. A. Abdel-Jawad, "The relationships of cement hydration and concrete compressive strength to maturity," PhD thesis, Univ. of Michigan, 1988.
[27] K. O. Kjellsen and R. J. Detwiler, "Reaction kinetics of portland cement mortar hydrated at different temperatures," *Cem. Concr. Res.*, vol. 22, no. 1, pp. 112–120, 1990.
[28] S. Jalali and M. Y. Abyaneh, "Prediction of final concrete strength in hot climates," *Magazine of Concrete Research*, vol. 47, no. 173, pp. 291-297, 1995.
[29] P. P. Hansen and E. J. Pedersen, "Curing of concrete structure," Report prepared for CEB—General Task Group No. 20, Danish Concrete and Structural Research Institute, Dec. 1984.
[30] I. Odler, *et al*., *CCR*, vol. 2, pp. 577-589, 1972.
[31] B. Kroone, *et al*., 1961, MCR, 13, No. 39, pp. 127-132.
[32] J. Shi-Ping, *et al*., *eeR*, vol. 19, no. 3, pp. 487-496, 1989.
[33] R. Trettin, *et al*., *7th ICCC*, Paris, vol. 4, pp. 163-167, 1980.
[34] A. Susanto, D. A. Koleva, E. A. B. Koenders, and K. van Breugel, "The effect of temperature rise on microstructural properties of cement-based materials: HYMOSTRUC3D modeling incorporating an 'electrical enhancement' factor," European Corrosion Congress (EUROCORR), Graz, Austria, 6-10 September 2015.

[35] D. P. Bentz, "Three-dimensional computer simulation of Portland cement hydration and microstructure development," *J. Am. Ceram. Soc*., vol. 80, no. 1, pp. 3–21, 1997.
[36] S. Goto and D. M. Roy, "The effect of W/C ratio and curing temperature on the permeability of hardened cement paste," *Cement Concrete Res*., vol. 11, no. 4, pp. 575–579, 1981.
[37] A. Bentur, *et al*., *JACS*, vol. 62, no. 7-8, pp. 362-366, 1979.

**A. Susanto** received Bachelor of Sciences from Department of Physics in 2001 at Institute of Technology Bandung (ITB), Indonesia. He continued his study at Instrumentation and Control Engineering, Department of Engineering Physics, ITB. During master study, he visited Kasai Laboratory, Division of Precision Science & Technology and Applied Physics, Osaka University, Osaka, Japan for a year (2003-2004), as an exchange student and finished his master thesis. In February 2011, he started his Ph.D research in Microlab, Material and Environment, Faculty of Civil Engineering and Geosciences, Delft University of Technology (TU Delft), The Netherlands.

**D.A. Koleva** is an assistant Professor at Faculty of Civil Engineering and Geosciences, Delft University of Technology, Section of Materials and Environment, The Netherlands.

**K. van Breugel** is Professor at Faculty of Civil Engineering and Geosciences, Delft University of Technology, Section of Materials and Environment, The Netherlands.